Continuum kinetic schemes for Vlasov-Maxwell equations, with applications to laboratory and space plasmas

Ammar H. Hakim[1] J. Juno[2] P. Cagas[3] J. TenBarge[2]
B. Srinivasan[3]

[1]Princeton Plasma Physics Laboratory, Princeton, NJ

[2]University of Maryland, MD

[3]Virgina Tech, VA

Theory Seminar, June 2017

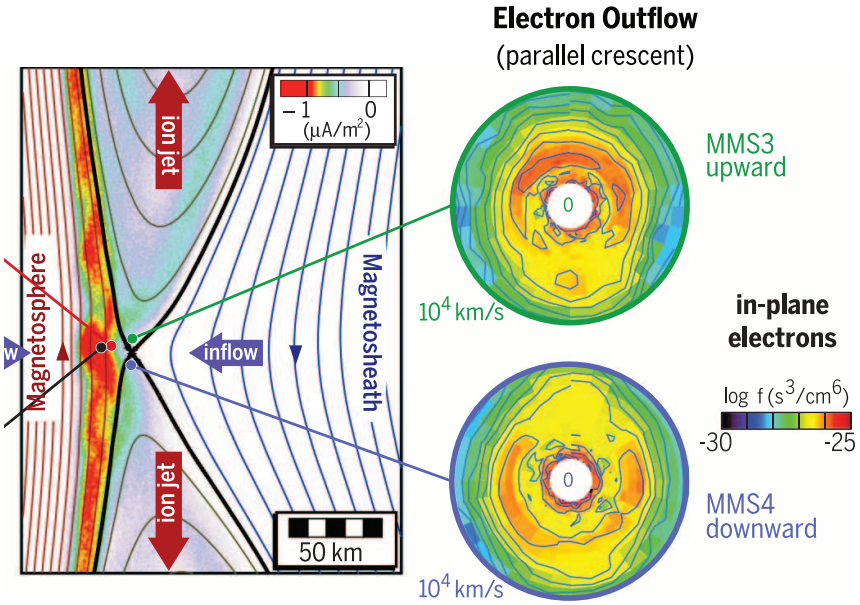

Magnetospheric Mutiscale (MMS) Mission

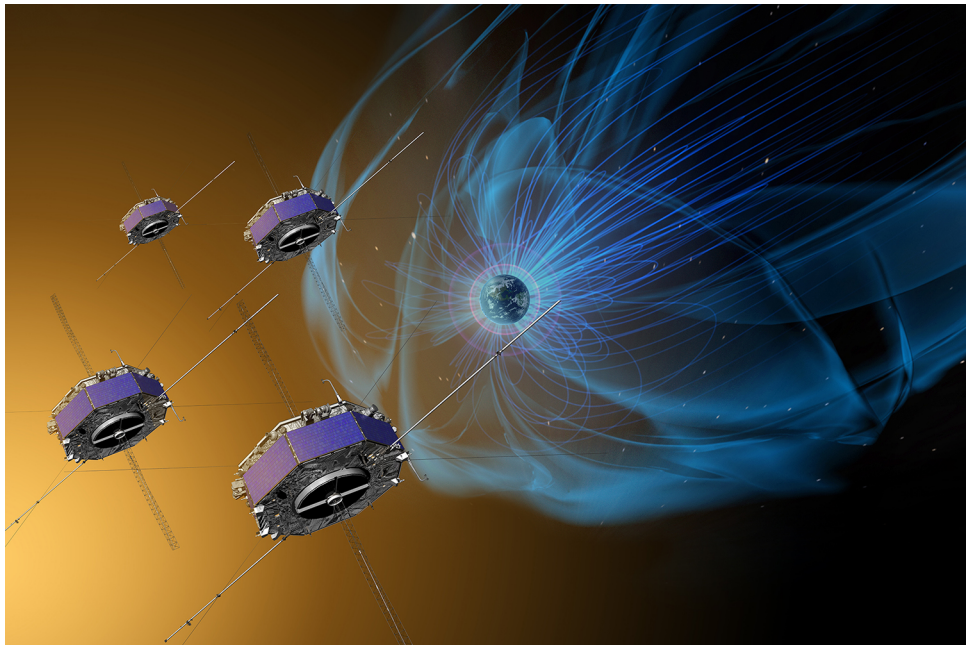

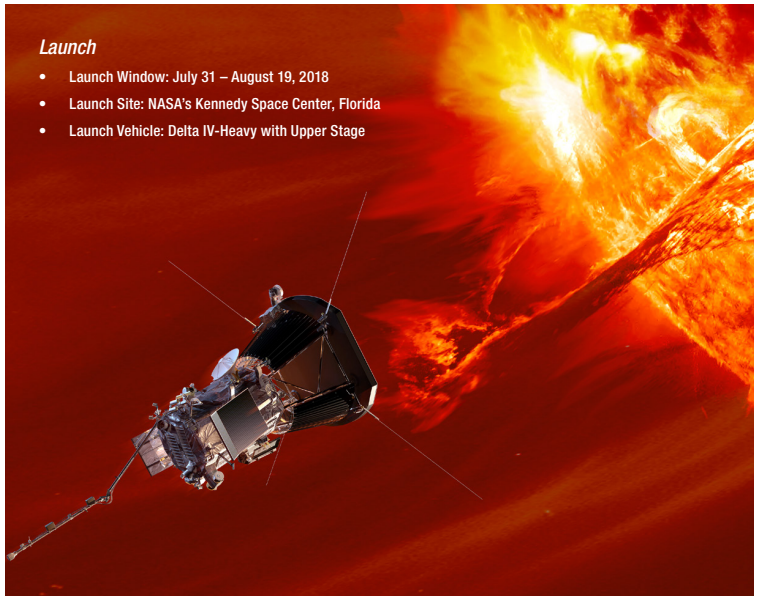

Parker Solar-Probe Plus Mission

- Determine the structure and dynamics of plasma at the sources of the solar wind
- Explore mechanisms that accelerate and transport energetic particles

FLARE Experiment at PPPL

- FLARE will provide detailed measurements of magnetic fields and other quantities down to electron scales during magnetic reconnections
- Important data to understand kinetic processes in reconnection and energetic particles

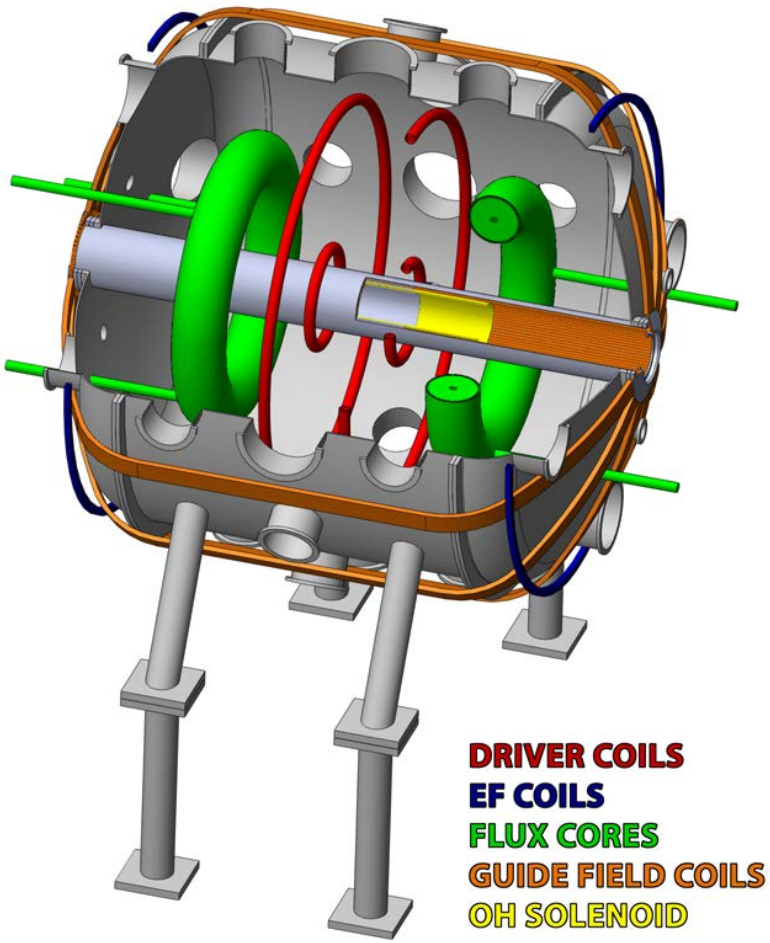

Non-plasma application: The GAIA mission is collecting position and velocity of 1% of stars in our galaxy: Can Vlasov models provide an alternate tool to N-body code to study structure formation in self-gravitating systems?

Goal: Understand kinetic physics in plasma from first-principles

We would like to solve the Vlasov-Maxwell system, treating it as a partial-differential equation (PDE) in 6D:

$$\frac{\partial f_s}{\partial t} + \nabla_{\mathbf{x}} \cdot (\mathbf{v} f_s) + \nabla_{\mathbf{v}} \cdot (\mathbf{F}_s f_s) = 0$$

where $\mathbf{F}_s = q_s/m_s(\mathbf{E} + \mathbf{v} \times \mathbf{B})$. The EM fields are determined from Maxwell equations

$$\frac{\partial \mathbf{B}}{\partial t} + \nabla \times \mathbf{E} = 0$$

$$\epsilon_0 \mu_0 \frac{\partial \mathbf{E}}{\partial t} - \nabla \times \mathbf{B} = -\mu_0 \mathbf{J}$$

Question: Can we solve the VM system *efficiently* while conserving important invariants?

We know that the Vlasov-Maxwell system conserves, total number of particles; total (field + particle) momentum; total (field + particle) energy; other invariants. Can a numerical scheme be designed that retains (some or all) of these properties?

For understanding solar-wind turbulence and other problems, we would like a noise-free algorithm that allows studying phase-space cascades correctly, in a noise-free manner.

Proposed answer: Explore high-order discontinuous Galerkin algorithms to directly discretize the Vlasov-Maxwell system.

Discontinuous Galerkin algorithms represent state-of-art for solution of hyperbolic partial differential equations

- DG algorithms hot topic in CFD and applied mathematics. First introduced by Reed and Hill in 1973 for neutron transport in 2D.
- General formulation in paper by Cockburn and Shu, JCP 1998. More than 700 citations.
- DG combines key advantages of finite-elements (low phase error, high accuracy, flexible geometries) with finite-volume schemes (limiters to produce positivity/monotonicity, locality)
- Certain types of DG have excellent conservation properties for, low noise and low dissipation.
- DG is inherently super-convergent: in FV methods interpolate p points to get pth order accuracy. In DG interpolate p points to get $2p-1$ order accuracy.

DG combined with FV schemes can lead to best-in-class explicit algorithms for hyperbolic PDEs.

Essential idea of Galerkin methods: L_2 minimization of errors on a finite-dimensional subspace

Consider a general time-dependent problem

$$f'(x,t) = G[f]$$

where $G[f]$ is some operator. To approximate it expand $f(x)$ with a finite set of basis functions $w_k(x)$,

$$f(x,t) \approx f_h(x,t) = \sum_{k=1}^{N} f_k(t) w_k(x)$$

This gives discrete system

$$\sum_{k=1}^{N} f'_k w_k(x) = G[f_h]$$

How to determine f'_k in an optimum manner?

Essential idea of Galerkin methods: L_2 minimization of errors on a finite-dimensional subspace

Answer: Do an L_2 minimization of the error, i.e. find f_k' such that

$$E_N = \int \left[\sum_{k=1}^{N} f_k' w_k(x) - G[f_h] \right]^2 dx$$

is minimum. For minimum error $\partial E_N / \partial f_m' = 0$ for all $k = 1, \ldots, N$. This leads to the linear system that determines the coefficients f_k'

$$\int w_m(x) \left(\sum_{k=1}^{N} f_k' w_k(x) - G[f_h] \right) dx = 0$$

for all $m = 1, \ldots, N$.
Projection of residual on the basis set chosen for expansion leads to minimum errors in the L_2 sense. For this reason DG/CG schemes are constructed by projecting residuals of PDEs on basis sets.

What does a typical L_2 fit look like for discontinuous Galerkin scheme?

Discontinuous Galerkin schemes use function spaces that allow *discontinuities* across cell boundaries.

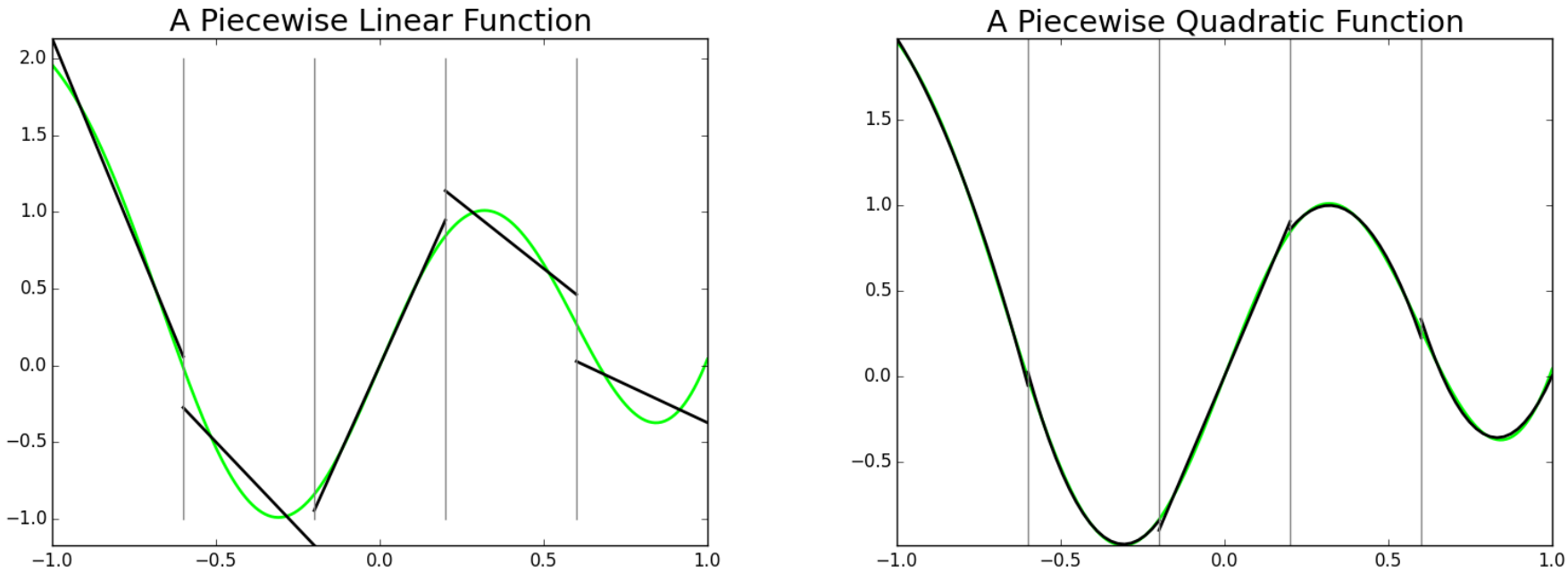

Figure: The best L_2 fit of $x^4 + \sin(5x)$ with piecewise linear (left) and quadratic (right) basis functions.

Passive advection is a good prototype to study DG schemes

Consider the 1D passive advection equation on $I \in [L, R]$

$$\frac{\partial f}{\partial t} + \lambda \frac{\partial f}{\partial x} = 0$$

with λ the constant advection speed. $f(x,t) = f_0(x - \lambda t)$ is the exact solution, where $f_0(x)$ is the initial condition. Designing a good scheme is much harder than it looks.

- Discretize the domain into elements $I_j \in [x_{j-1/2}, x_{j+1/2}]$
- Pick a finite-dimensional function space to represent the solution. For DG we usually pick polynomials in each cell but allow discontinuities across cell boundaries
- Expand $f(x,t) \approx f_h(x,t) = \sum_k f_k(t) w_k(x)$.

Passive advection is harder than it looks: Excerpt from 1978 paper!

The linear advective equation

$$\frac{\partial u}{\partial t} + v \frac{\partial u}{\partial x} = 0$$

is the simplest imaginable PDE, and the great difficulty of solving it numerically causes considerable embarrassment to those attempting to solve complex PDE systems. However, it does provide a good case

Discrete problem can be stated as finding the coefficients that minimize the L_2 norm of the residual

The discrete problem in DG is stated as: find f_h in the function space such that for each basis function φ we have

$$\int_{I_j} \varphi \left(\frac{\partial f_h}{\partial t} + \lambda \frac{\partial f_h}{\partial x} \right) \, dx = 0.$$

Integrating by parts leads to the discrete *weak-form*

$$\int_{I_j} \varphi \frac{\partial f_h}{\partial t} \, dx + \lambda \varphi_{j+1/2} \hat{f}_{hj+1/2} - \lambda \varphi_{j-1/2} \hat{f}_{hj-1/2} - \int_{I_j} \frac{d\varphi}{dx} \lambda f_h \, dx = 0.$$

Here $\hat{f}_h = \hat{f}(f_h^+, f_h^-)$ is the consistent *numerical flux* on the cell boundary. Integrals are performed using high-order quadrature schemes.

Picking a good numerical flux is key to stability, accuracy

- Take averages

$$\hat{f}_h(f_h^+, f_h^-) = \frac{1}{2}(f_h^+ + f_h^-)$$

- Use upwinding

$$\begin{aligned}\hat{f}_h(f_h^+, f_h^-) &= f_h^- \quad \lambda > 0 \\ &= f_h^+ \quad \lambda < 0\end{aligned}$$

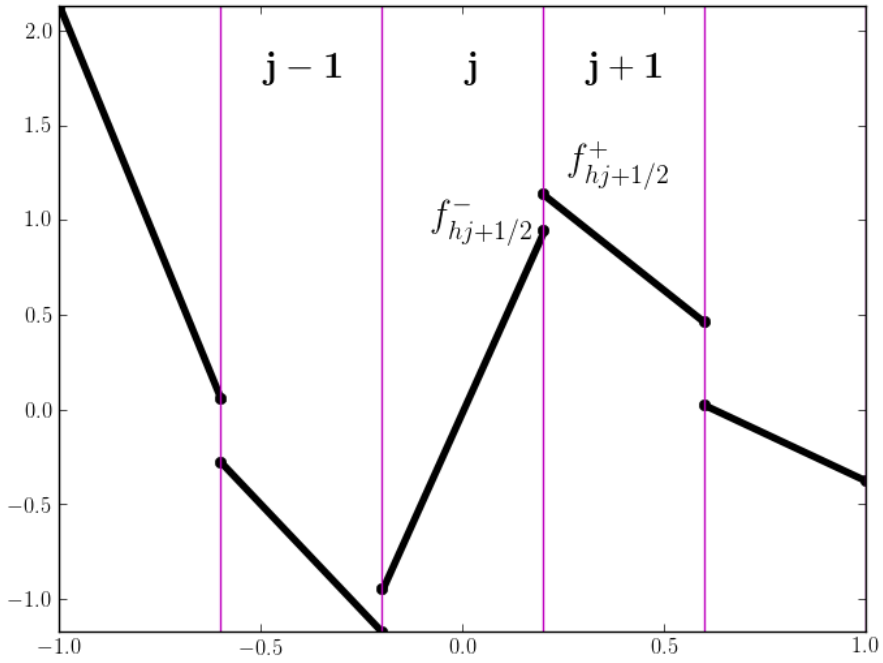

For system of nonlinear equations (Euler, ideal MHD, etc.) there is cottage industry on choosing numerical fluxes. Google "Riemann solvers"

Example: Piecewise constant basis functions lead to familiar difference equations

- A central flux with piecewise constant basis functions leads to the familiar central difference scheme

$$\frac{\partial f_j}{\partial t} + \lambda \frac{f_{j+1} - f_{j-1}}{2\Delta x} = 0$$

- An upwind flux with piecewise constant basis functions leads to the familiar upwind difference scheme (for $\lambda > 0$)

$$\frac{\partial f_j}{\partial t} + \lambda \frac{f_j - f_{j-1}}{\Delta x} = 0$$

Solution is advanced in time using a suitable ODE solver, usually strong-stability preserving Runge-Kutta methods.

Example: Piecewise constant basis functions with central flux leads to dispersive errors

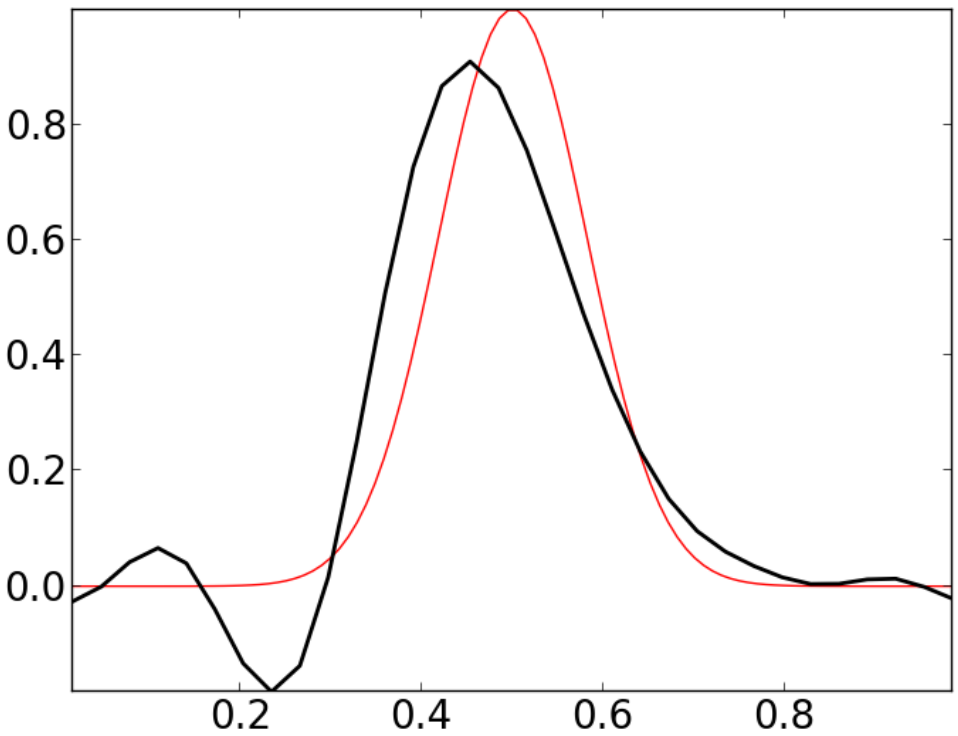

Figure: Advection equation solution (black) compared to exact solution (red) with central fluxes and piecewise constant basis functions.

Example: Piecewise constant basis functions with upwind flux is very diffusive

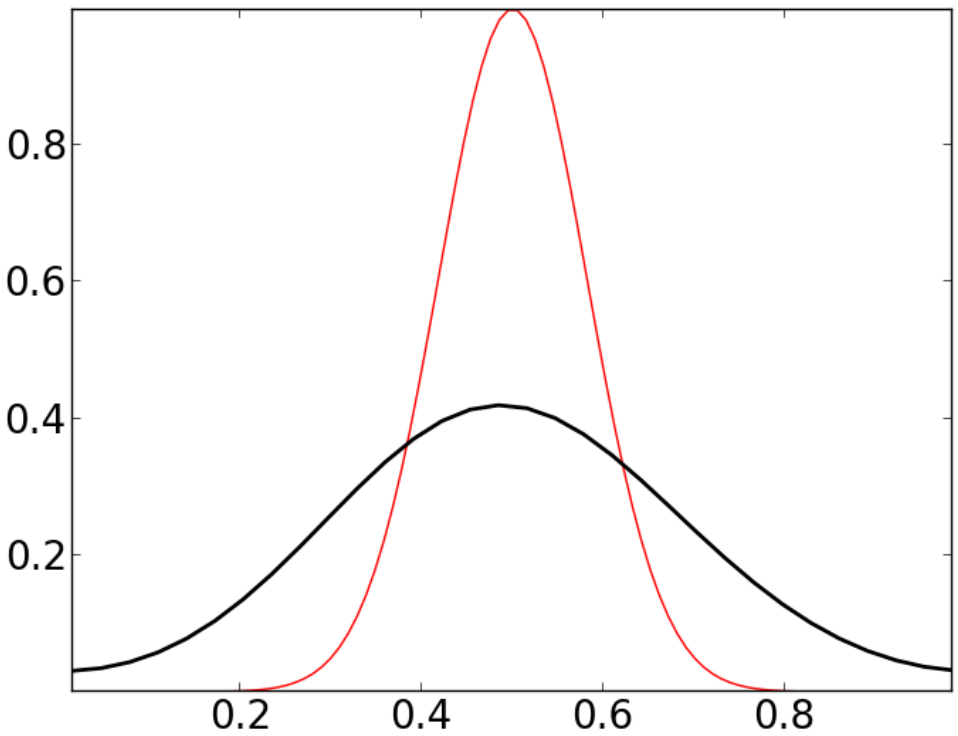

Figure: Advection equation solution (black) compared to exact solution (red) with upwind fluxes and piecewise constant basis functions.

Example: Piecewise linear space with upwind flux leads to good results

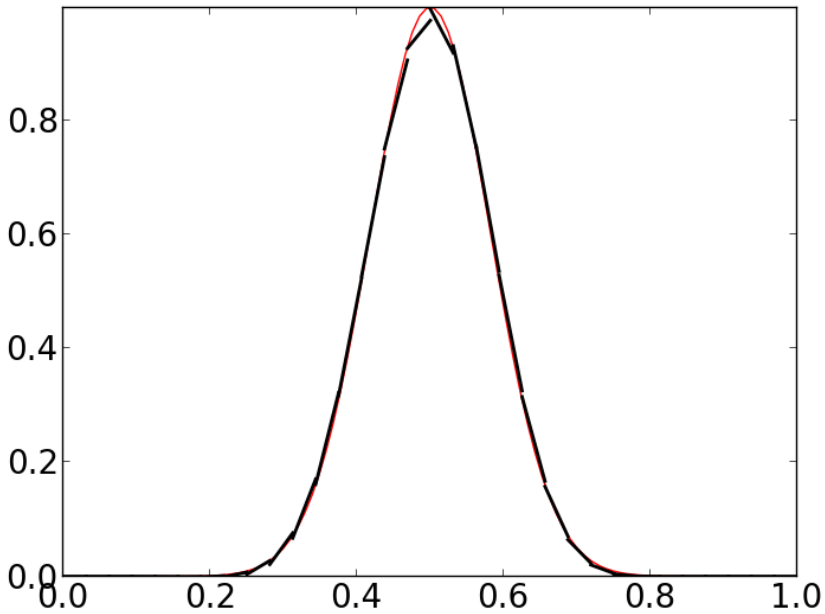

Figure: Advection equation solution (black) compared to exact solution (red) with upwind fluxes and piecewise linear basis functions.

In general, with upwind fluxes and linear basis functions numerical diffusion goes like $|\lambda|\Delta x^3 \partial^4 f/\partial x^4$.

Summary of DG schemes

- Pick basis functions. These are usually piecewise polynomials, but could be other suitable functions.
- Construct discrete weak-form using integration by parts.
- Pick suitable numerical fluxes (Riemann solvers) for the surface integrals.
- Pick a suitable quadrature scheme to perform surface and volume integrals.
- Use Runge-Kutta (or other suitable) schemes for evolving the equations in time.

Other major topics in DG: limiters for positivity/monotonicity, nodal vs. modal basis functions, Serendipity basis functions, diffusion terms, general geometry, error and accuracy analysis, hp-refinement, etc.

We use DG for both Vlasov and Maxwell equations

Start from Vlasov equation written as advection equation in phase-space:

$$\frac{\partial f_s}{\partial t} + \nabla_{\mathbf{z}} \cdot (\boldsymbol{\alpha} f_s) = 0$$

where advection velocity is given by $\boldsymbol{\alpha} = (\mathbf{v}, q/m(\mathbf{E} + \mathbf{v} \times \mathbf{B}))$.

To derive the semi-discrete Vlasov equation using a discontinuous Galerkin algorithm, we introduce phase-space basis functions $w(\mathbf{z})$, and derive the discrete scheme:

$$\int_{K_j} w \frac{\partial f_h}{\partial t} \, d\mathbf{z} + \oint_{\partial K_j} w^- \mathbf{n} \cdot \hat{\mathbf{F}} \, dS - \int_{K_j} \nabla_{\mathbf{z}} w \cdot \boldsymbol{\alpha}_h f_h \, d\mathbf{z} = 0$$

We use DG for both Vlasov and Maxwell equations

Multiply Maxwell equations by basis φ and integrate over a cell. We have terms like

$$\int_{\Omega_j} \underbrace{\varphi \nabla \times \mathbf{E}}_{\nabla\times(\varphi\mathbf{E})-\nabla\varphi\times\mathbf{E}} \; d^3\mathbf{x}.$$

Gauss law can be used to convert one volume integral into a surface integral

$$\int_{\Omega_j} \nabla \times (\varphi \mathbf{E}) \, d^3\mathbf{x} = \oint_{\partial\Omega_j} d\mathbf{s} \times (\varphi \mathbf{E})$$

Using these expressions we can now write the discrete weak-form of Maxwell equations as

$$\int_{\Omega_j} \varphi \frac{\partial \mathbf{B}_h}{\partial t} \, d^3\mathbf{x} + \oint_{\partial\Omega_j} d\mathbf{s} \times (\varphi^- \hat{\mathbf{E}}_h) - \int_{\Omega_j} \nabla\varphi \times \mathbf{E}_h \, d^3\mathbf{x} = 0$$

$$\epsilon_0\mu_0 \int_{\Omega_j} \varphi \frac{\partial \mathbf{E}_h}{\partial t} \, d^3\mathbf{x} - \oint_{\partial\Omega_j} d\mathbf{s} \times (\varphi^- \hat{\mathbf{B}}_h) + \int_{\Omega_j} \nabla\varphi \times \mathbf{B}_h \, d^3\mathbf{x} = -\mu_0 \int_{\Omega_j} \varphi \mathbf{J}_h \, d^3\mathbf{x}.$$

Example basis functions: Serendipity elements

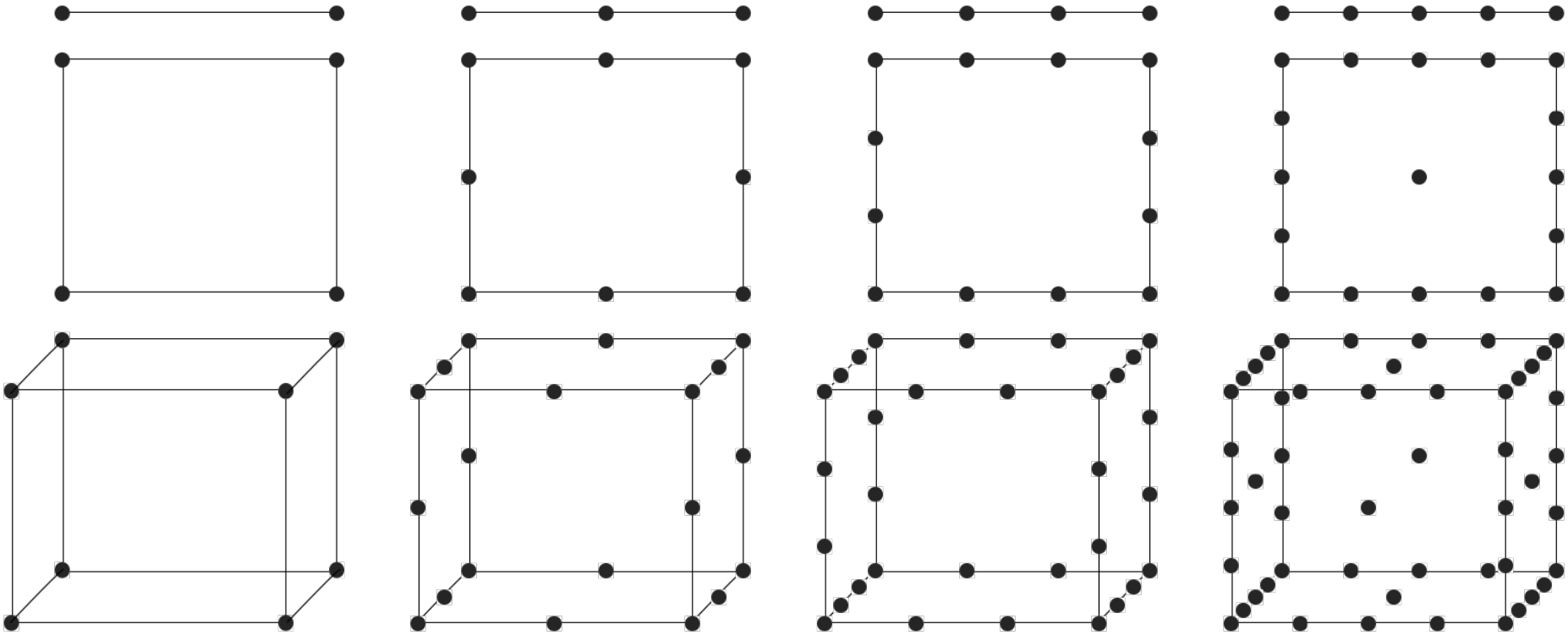

Figure: Schematic drawing of the nodal locations for the Serendipity basis in 1D (top), 2D (middle), and 3D (bottom) for polynomial orders one (far left), two (middle left), three (middle right), and four (far right).

Is energy conserved? Are there any constraints on basis functions/numerical fluxes?

Answer: Yes! If one is careful. We want to check if

$$\frac{d}{dt}\sum_j\sum_s\int_{K_j}\frac{1}{2}m|\mathbf{v}|^2 f_h\,d\mathbf{z} + \frac{d}{dt}\sum_j\int_{\Omega_j}\left(\frac{\epsilon_0}{2}|\mathbf{E}_h|^2 + \frac{1}{2\mu_0}|\mathbf{B}_h|^2\right)d^3\mathbf{x} = 0$$

Proposition

If central-fluxes are used for Maxwell equations, and if $|\mathbf{v}|^2$ is projected to the approximation space, the semi-discrete scheme conserves total (particles plus field) energy exactly.

The proof is rather complicated, and needs careful analysis of the discrete equations (See Juno et. al. arXiv:1705.05407)

Remark

If upwind fluxes are used for Maxwell equations, the total energy will decay monotonically. Note that the energy conservation does not depend on the fluxes used to evolve Vlasov equation.

Is momentum conserved?

Answer: No. Errors in momentum come about due to discontinuity in electric field at cell interfaces. However, *momentum conservation errors are independent of velocity space discretization, and drop rapidly with increasing configuration space resolution*.

Fully discrete system conserves energy/momentum extremely well

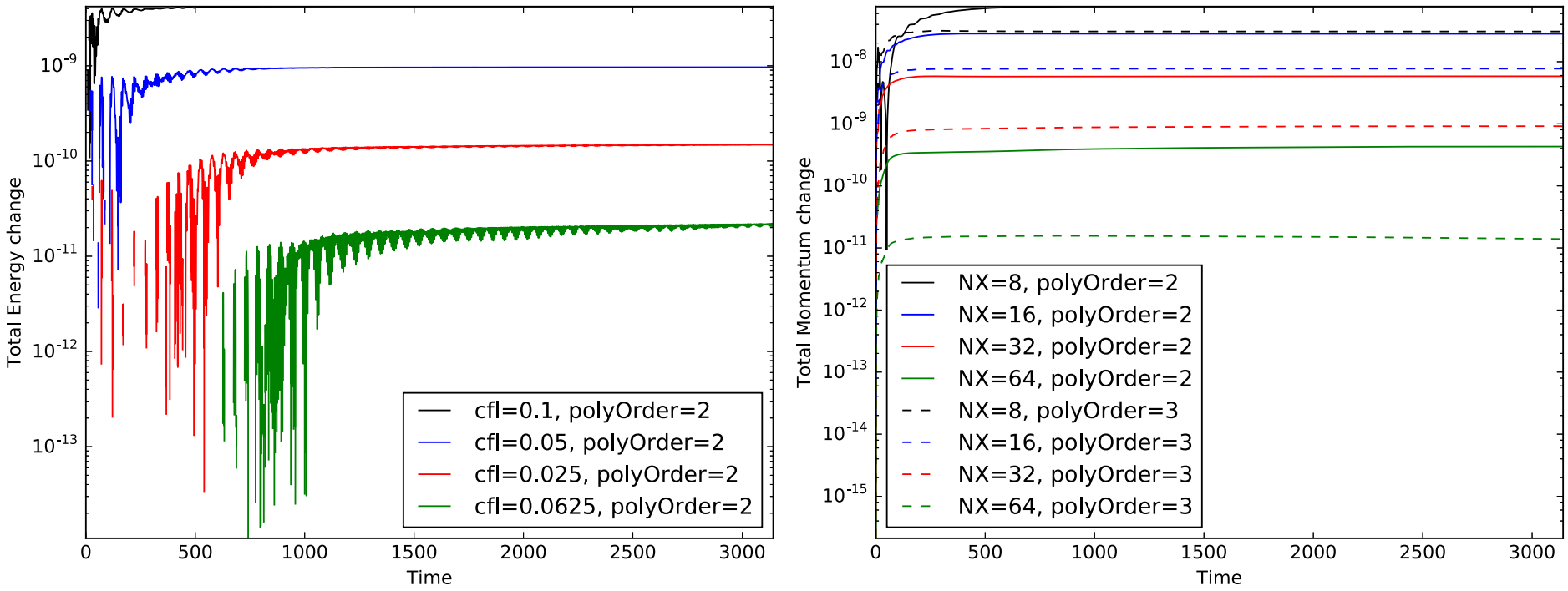

Figure: Left plot is the relative change in the total energy and right plot is the relative change in the total (proton and electron) momentum.

To give and not to count the cost ...

Question: Are continuum schemes competitive compared to PIC schemes in terms of cost for a given accuracy?

I am not completely sure and it probably depends on what you are looking for.

In general, if one is interested in detailed phase-space structure of distribution function, then continuum scheme can be very efficient as the lack of noise allows interpretation of data (for turbulence, for example) easier.

Our recent algorithmic innovations in constructing special basis sets has shown that continuum schemes can be made to scale as number of basis functions in phase-space. (In standard DG, the schemes usually scale quadratically or cubially with number of basis functions!). This is potentially a game-changer as efficiency improves dramatically (at the cost of more complex code).

Algorithms implemented in Gkeyll code

"It is one thing to mortify curiosity, another to conquer it"

- Gkeyll framework is a flexible suite of solvers for plasma physics; written in Lua with backend in C++
- Solvers for gyrokinetic, Vlasov-Maxwell, multifluid equations in same package
- Open-source and executable available via Anaconda package manager (coming soon)

We have performed verification tests and initial physics study

Electrostatic Shocks (1X/1V)

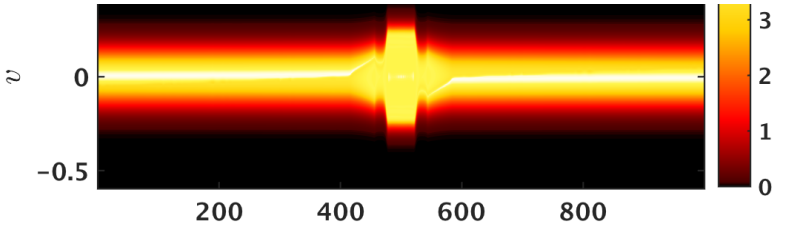

Kinetic Saturation of Weibel Instability

Cagas et. al. arXiv:1705.07930

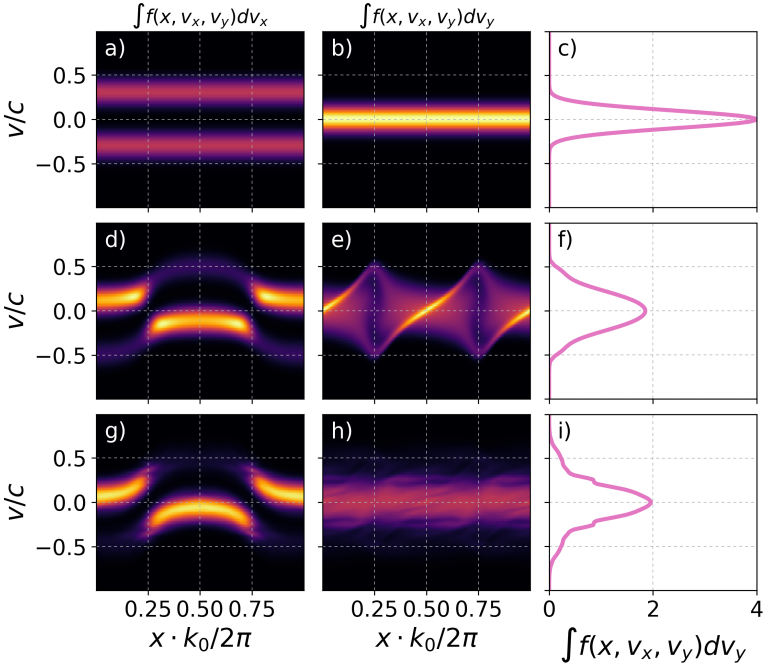

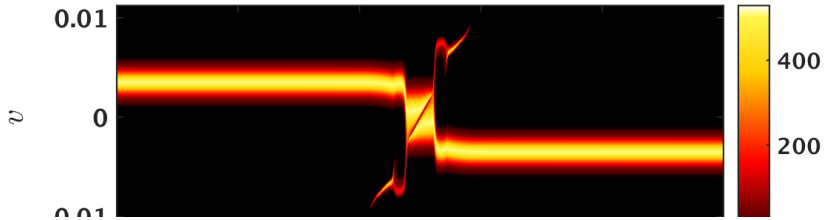

Orsang-Tang Vortex (2X/3V)

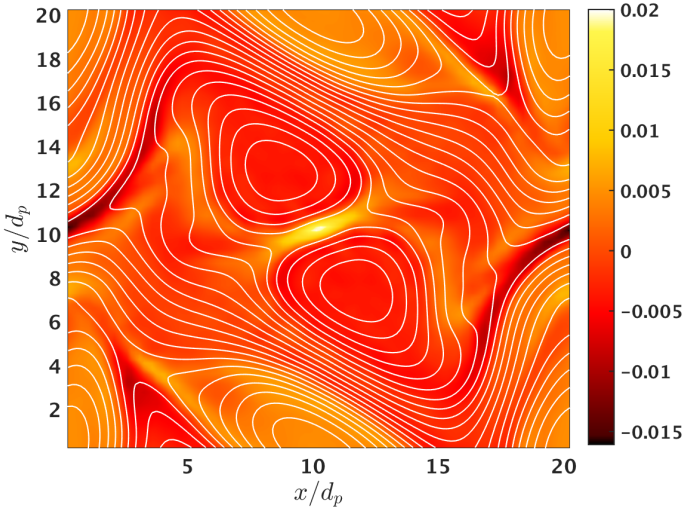

See Juno et. al. arXiv:1705.05407

Application 1: What is the mechanism for saturation of Weibel instability?

Leading mechanism for the origin and growth of magnetic fields in a number of laboratory and astrophysical plasma applications

Analytical dispersion relation:

$$\frac{1}{2} = \frac{\omega_0^2}{c^2 k^2}\left[\zeta Z(\zeta)\left(1+\frac{v_D^2}{v_{th}^2}\right)+\frac{v_D^2}{v_{th}^2}\right]+\frac{v_{th}^2}{c^2}\zeta^2,$$

WI/CFI growth

Under-prediction for higher k – possible explanation through temperature increase (more details later)

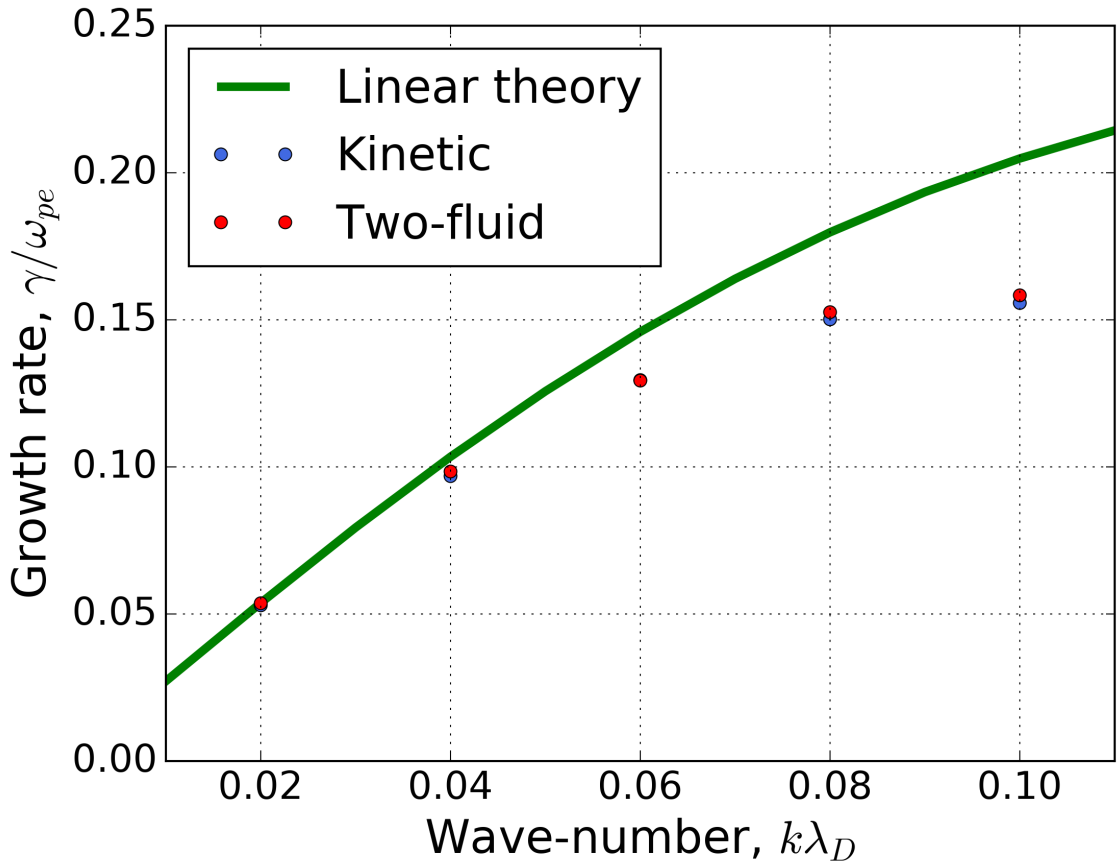

WI/CFI saturation

Nonlinear saturation traditionally contributed to magnetic trapping

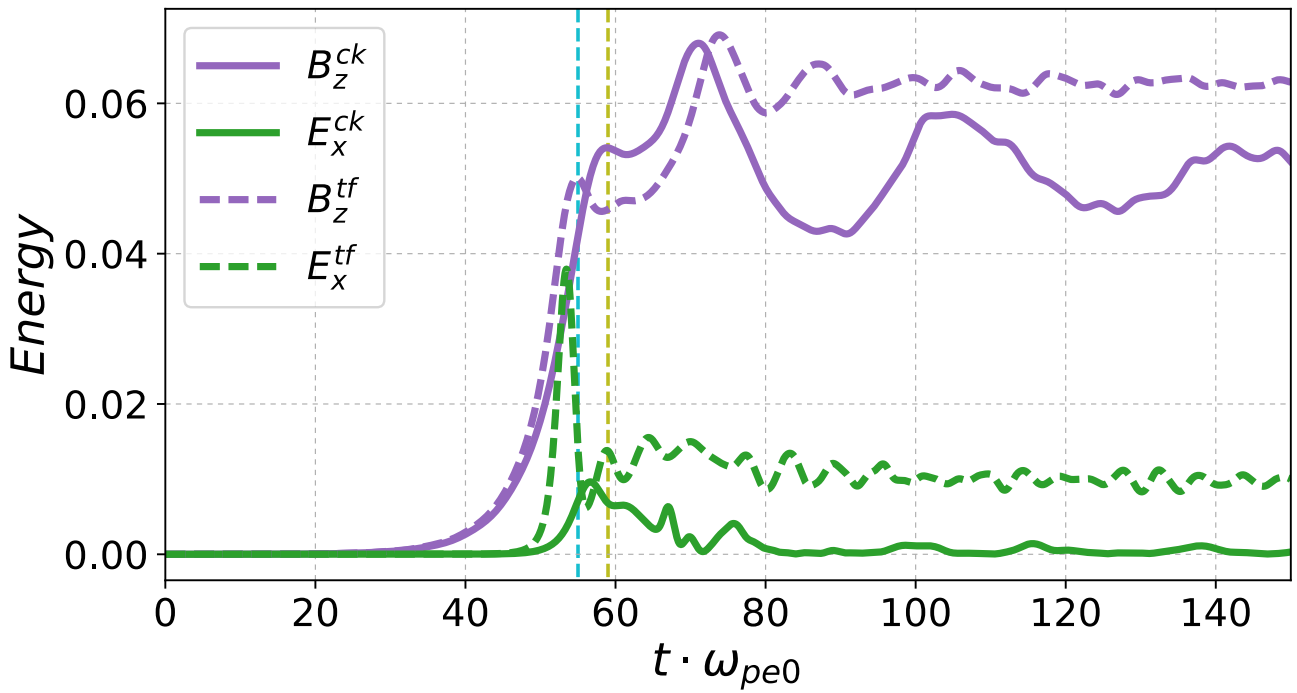

Note the correspondence of the magnetic field saturation with the the saturation of electric field

Interplay between electric and magnetic fields

Initial conditions – two counterstreaming populations

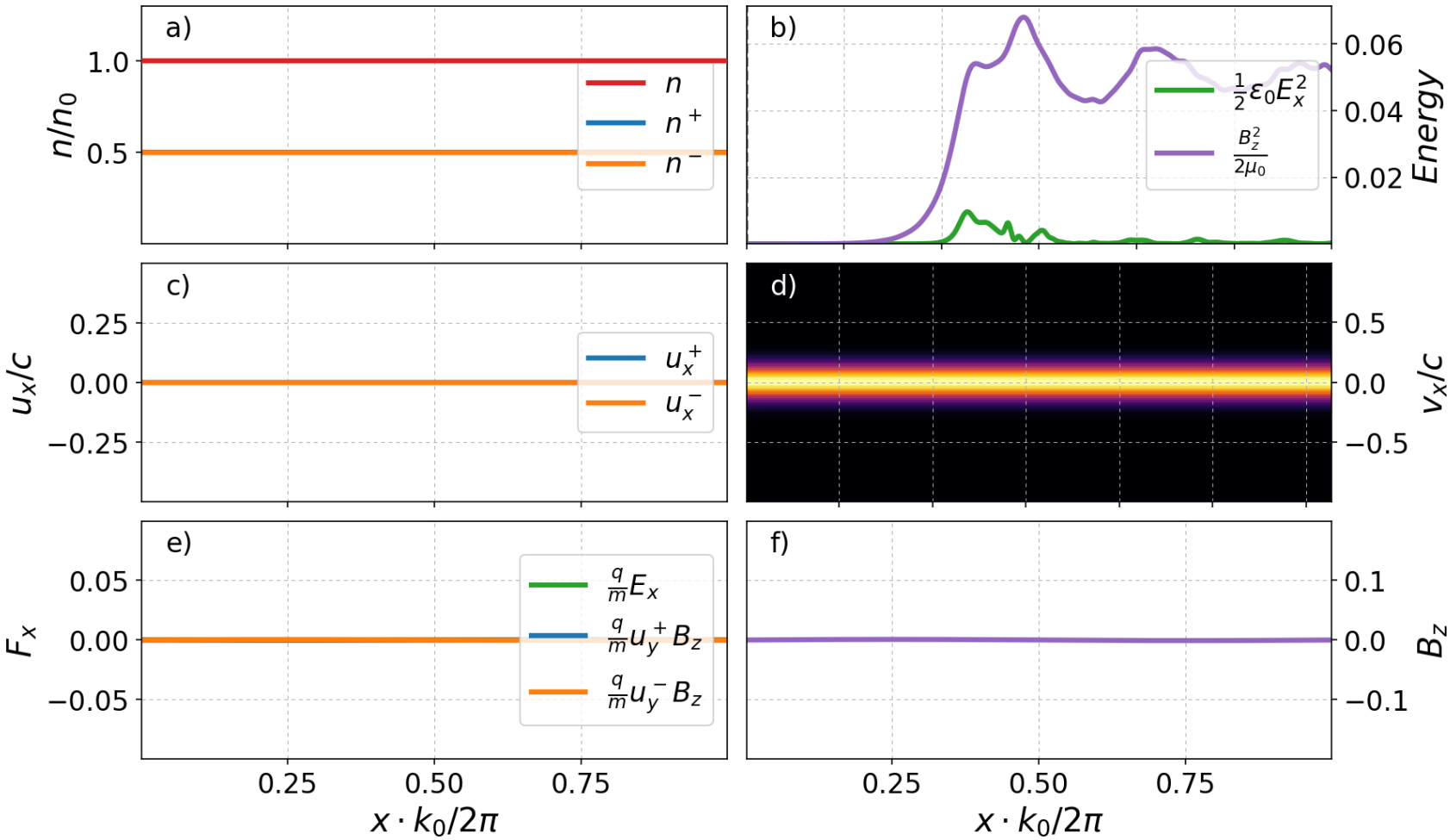

Interplay between electric and magnetic fields

Filamentation is apparent; counterstreaming starts in v_x

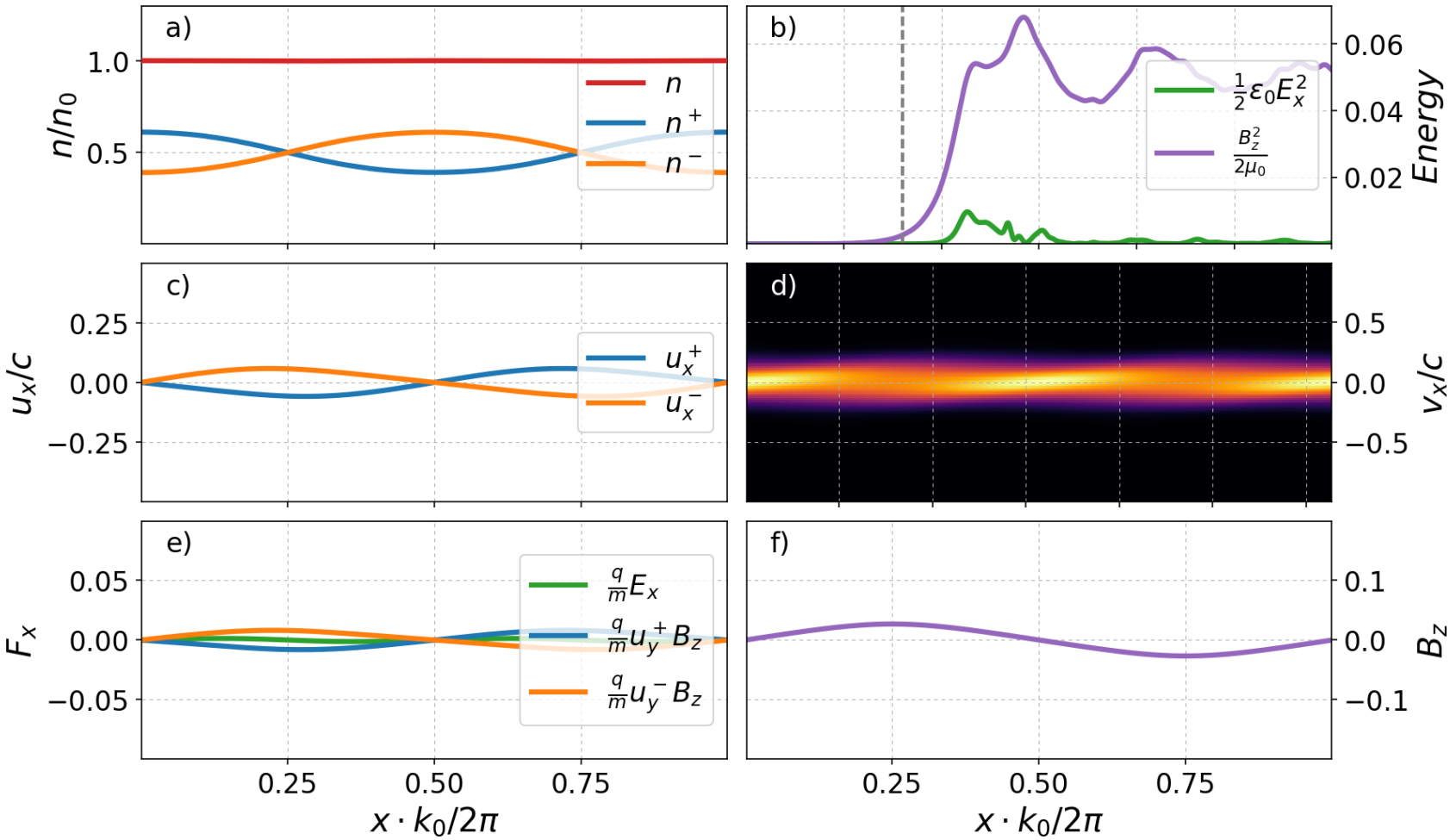

Interplay between electric and magnetic fields

Collapse of the secondary instability; v_x flow reversal

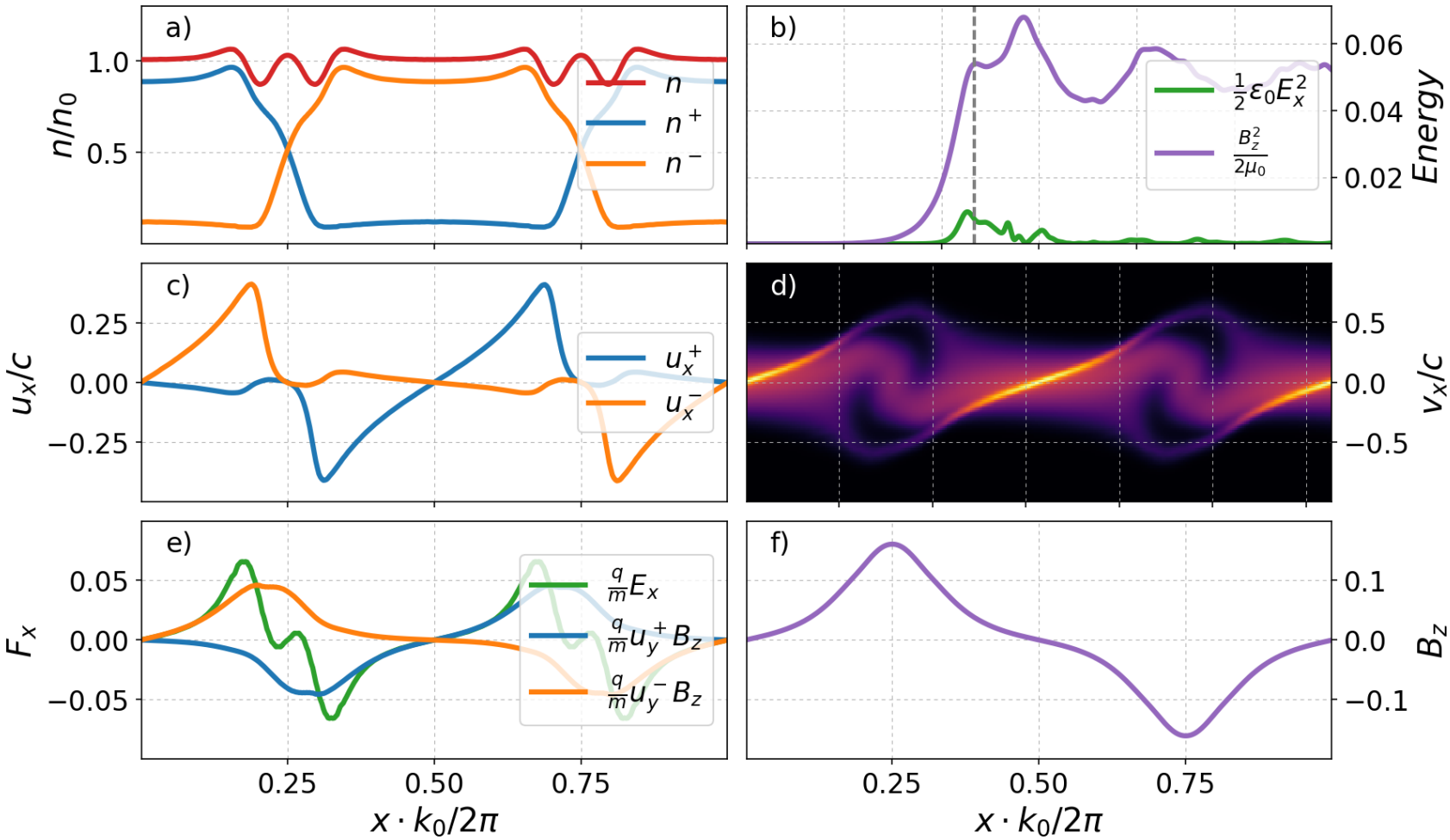

Interplay between electric and magnetic fields

v_x flow reversed; magnetic field energy decreasing

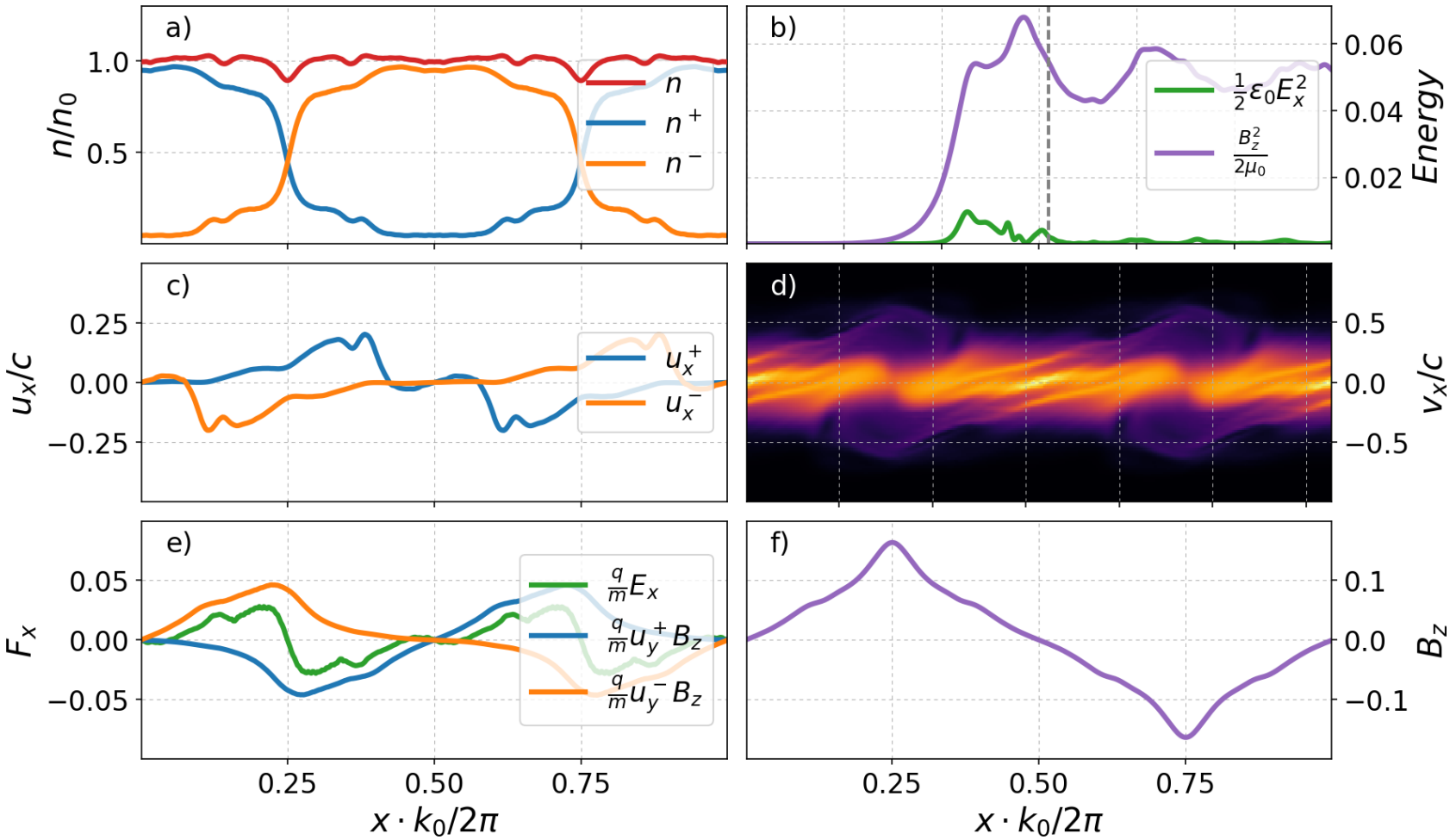

Periodic "predator-prey" behavior

1. Secondary instability hinders the filamentation and with it magnetic field growth
2. Reversal of the flow after the collapse of the secondary instability decreases magnetic field
3. Filamentation force reintroduces the filamentation v_x flow
4. Secondary instability starts to grow

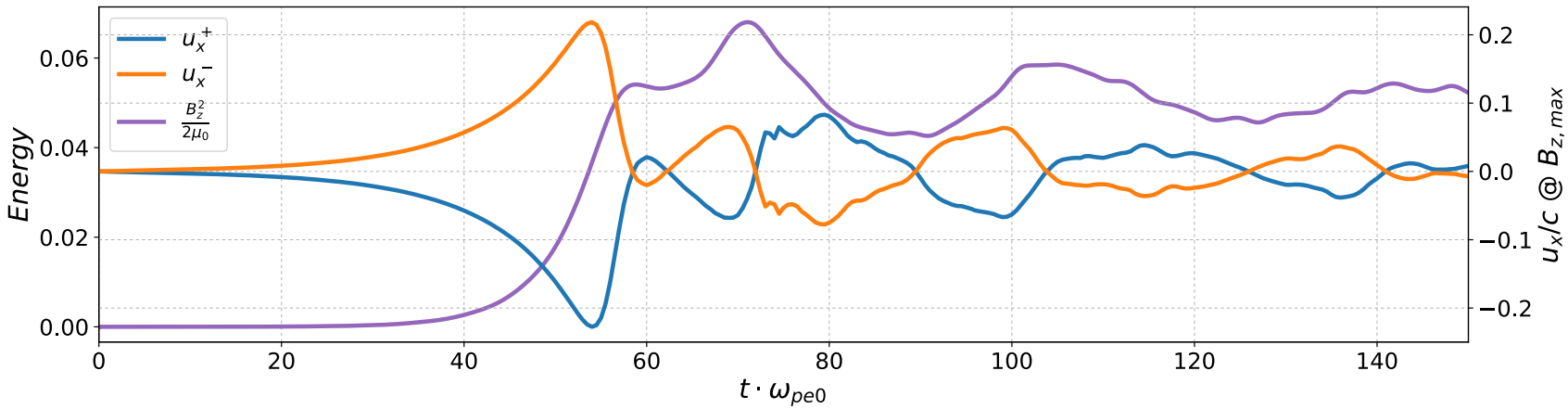

Distribution functions and heating

In order to show as 2D plots, distribution functions are integrated over v_x and v_y at the beginning of the simulation, after $59/\omega_{pe0}$ (time of the first saturation), and in the end $(150/\omega_{pe0})$

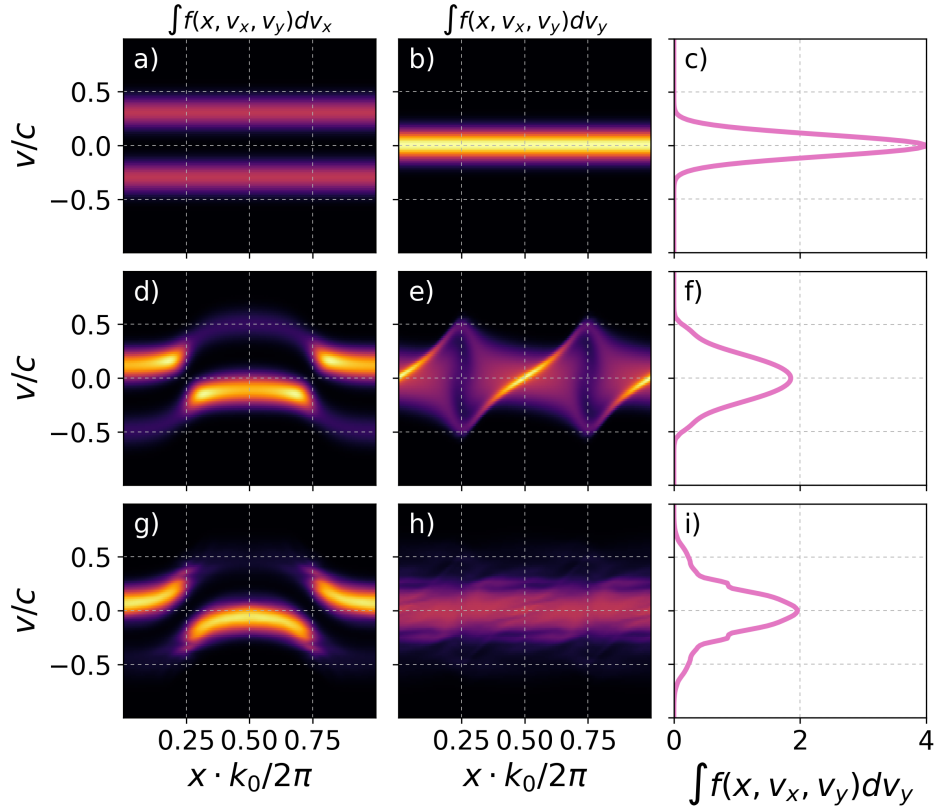

Application 2: 2D turbulence in magnetized plasmas

We have performed 2X/3V simulations of 2D turbulence in a magnetized plasma

Orszag-Tang initial conditions. Widely used to benchmark MHD codes and study physics of turbulence in 2D. We add a guide field of 5. $40 \times 40 \times 8^3$ mesh, with 112 nodes per cell. (90 million DOFs)

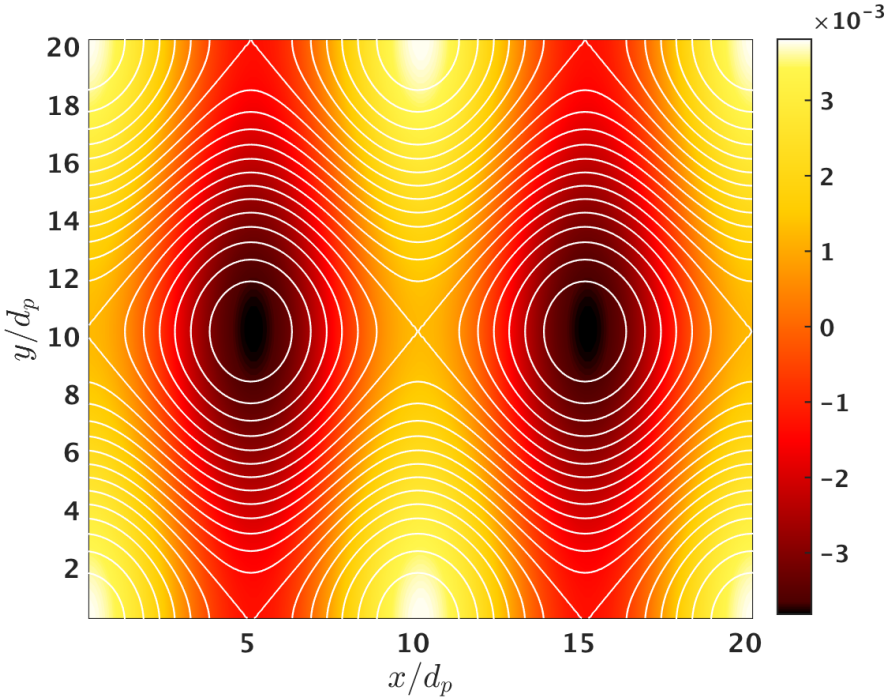

Figure: The out of plane current J_z with magnetic field contours superimposed

Energy spectrum of turbulence

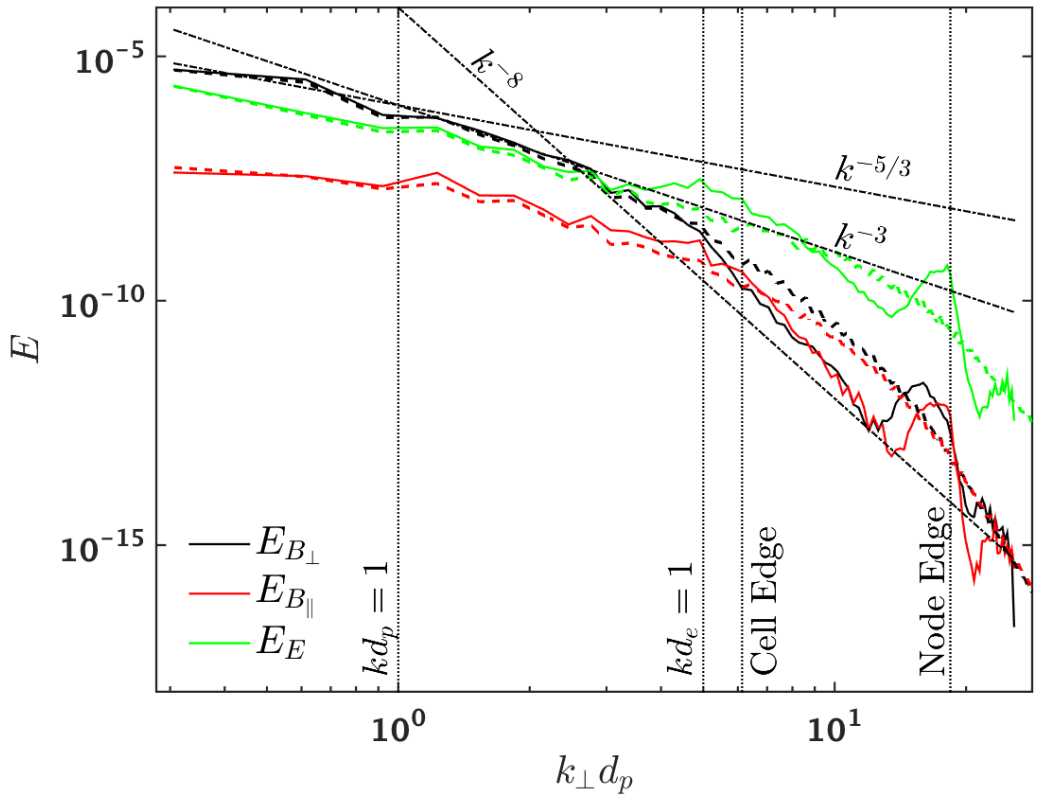

Figure: The energy spectra for Vlasov (solid lines) and 10 moment two fluid (dashed lines) at $t = 35\Omega_{cp}^{-1}$ of the Orszag-Tang vortex simulation. The perpendicular and parallel magnetic energy spectra are directions with respect to the magnetic field. The various slopes denote the fitted spectra at each of the spectral breaks. These compare well with previous results which suggest that at scales $kd_p < 1$, the spectra in $k_\perp$ is fitted by a -5/3 slope, before steepening at $kd_p > 1, kd_e < 1$, and steepening further at $kd_e > 1$.

Conclusion: We have developed a novel, energy conserving scheme Vlasov-Maxwell equations

- We have implemented a high-order discontinuous Galerkin algorithm for the solution of Vlasov-Maxwell equations
- Our algorithm conserves particles and energy exactly; momentum conservation is not exact, but is independent of velocity space resolution
- We have performed extensive benchmarks simulating basic plasma physics problems
- We have applied our algorithms to study physics of plasma shocks, Weibel instability and 2D plasma turbulence
- Current work is aimed towards improving performance via algorithmic improvements and code optimization
- We are beginning to explore detailed physics of plasma turbulence in solar wind
- Many basic plasma physics studies are possible! Come talk to me or Jimmy about possible topics for collaboration